

Marc Jerónimo Pérez y Roperó  
13-938-311

# Master Thesis

## Master's Thesis

Bachelor's Degree Programme in Environmental Sciences  
Physics of Soils and Terrestrial Ecosystems Group  
Swiss Federal Institute of Technology (ETH) Zurich

## Supervision

Prof. Dr. Emmanuel Frossard  
Dr. Frank Liebisch

## **Abstract**

Hier kommt das Abstract

Marc Jerónimo Pérez y Roperó  
13-938-311

# Master Thesis

## Master's Thesis

Bachelor's Degree Programme in Environmental Sciences  
Physics of Soils and Terrestrial Ecosystems Group  
Swiss Federal Institute of Technology (ETH) Zurich

## Supervision

Prof. Dr. Emmanuel Frossard  
Dr. Frank Liebisch

## Table of contents

<b>1</b>	<b>Abstract</b>	<b>5</b>
<b>2</b>	<b>Introduction</b>	<b>5</b>
2.1	The Complexity of Phosphorus . . . . .	5
2.2	From Static Measurements to Dynamic Understanding . . . . .	5
2.3	Objectives and Research Questions . . . . .	6
<b>3</b>	<b>Materials and Methods</b>	<b>6</b>
3.1	The Long-Term Phosphorus Fertilization Experiment . . . . .	6
3.2	Experimental Sites . . . . .	6
3.3	Phosphorus Desorption Kinetics . . . . .	7
3.3.1	Original Method of Flossmann and Richter (1982) {#sec-original-method-of-flossmann-and-richter-(1982)} . . . . .	7
3.3.2	Adapted Kinetic Protocol for This Study . . . . .	7
3.4	Statistical Analysis . . . . .	8
3.4.1	Modeling of Desorption Kinetics . . . . .	8
3.4.2	Modeling of Agronomic Responses . . . . .	9
<b>4</b>	<b>Results</b>	<b>10</b>
4.1	Establishment of the P-Desorption Kinetic Model . . . . .	10
4.1.1	Initial Approach: Failure of the Linearized Model . . . . .	10
4.1.2	Final Approach: Successful Non-Linear Model . . . . .	11
4.2	Comparison with Isotopic Exchange Kinetics (IEK) {#sec-comparison-with-isotopic-exchange-kinetics-(iek)} . . . . .	12
4.3	Effects of Fertilization on Agronomic and Soil Parameters . . . . .	13
4.3.1	Agronomic Responses to P Fertilization . . . . .	13
4.3.2	Soil P Parameters as a Function of P Fertilization . . . . .	15
4.4	Predicting P Parameters from Soil Properties . . . . .	16
4.5	Predictive Modeling of Agronomic Outcomes . . . . .	16
4.5.1	Predicting Site-Normalized Yield ( $Y_{norm}$ ) . . . . .	17
4.5.2	Predicting National-Normalized Yield ( $Y_{rel}$ ) . . . . .	17
4.5.3	Predicting P-Export ( $P_{up}$ ) . . . . .	17
4.5.4	Predicting P-Balance ( $P_{bal}$ ) . . . . .	18
<b>5</b>	<b>Discussion</b>	<b>19</b>
<b>6</b>	<b>Conclusion</b>	<b>19</b>
<b>7</b>	<b>Acknowledgments</b>	<b>19</b>
<b>8</b>	<b>Legal Disclosure</b>	<b>19</b>
<b>9</b>	<b>References</b>	<b>19</b>
<b>10</b>	<b>Appendix</b>	<b>19</b>
<b>11</b>	<b>Supplements</b>	<b>19</b>

## List of Figures

1	Flow-chart of the adapted Kinetik-experiment after Flossmann & Richter. . . . .	8
2	Test of the linearized first-order kinetic model. The plot visually supports the statistical finding that many intercepts are not zero. . . . .	11

3	Non-linear first-order kinetic model fits for P desorption over time. Points represent measured data and solid lines represent the fitted model for each replicate. . . . .	12
4	Correlation between desorption-derived kinetic parameters and IEK-derived parameters. (A) Capacity parameters: Desorbable P ( $P_{\text{desorb}}$ ) vs. Isotopically Exchangeable P ( $E_{7\text{d}}$ ). (B) Kinetic parameters: Rate Constant ( $k$ ) vs. IEK kinetic parameter ( $n_{1\text{d}}$ ). . . . .	13
5	Agronomic response variables across six P fertilization treatments and six experimental sites. Data from 2017-2022. . . . .	14
6	Soil P parameters across six P fertilization treatments and six experimental sites. . . . .	15

## List of Tables

1	Soil characteristics of the six long-term experimental sites. Data adapted from Hirte et al. (2021). . . . .	7
2	Description of variables used in the agronomic models. . . . .	9
3	Results of linear mixed-effects models predicting P parameters from intrinsic soil properties. Significance codes: “ $p < 0.001$ ,” “ $p < 0.01$ ,” “ $p < 0.05$ .” . . . .	16
4	Results of linear mixed-effects models predicting Site-Normalized Yield ( $Y_{\text{norm}}$ ). . . . .	17
5	Results of linear mixed-effects models predicting National-Normalized Yield ( $Y_{\text{rel}}$ ). . . . .	17
6	Results of linear mixed-effects models predicting P-Export ( $P_{\text{up}}$ ). . . . .	18
7	Results of linear mixed-effects models predicting P-Balance ( $P_{\text{bal}}$ ). . . . .	18

## 1 Abstract

## 2 Introduction

### 2.1 The Complexity of Phosphorus

Phosphorus (P) is an essential macronutrient for all known life, forming a critical part of DNA and energy-transfer molecules. In soils—where organic, mineral, and aqueous phases interface—its behavior is complex. In the presence of oxygen, P exists almost exclusively as orthophosphate ( $PO_4^{3-}$ ) and its protonated forms ( $HPO_4^{2-}$  or  $H_2PO_4^-$ ), depending on the soil pH. These dissolved phosphate species are highly reactive; they are subject to adsorption onto the surfaces of clays and oxides and can precipitate with cations like calcium, iron, and aluminum to form minerals with low solubility. Consequently, while the total amount of P in a soil can be large, only a small fraction is in the soil solution at any given moment, posing a central challenge for agriculture. The efficacy of P fertilization is often low due to these rapid immobilization processes, and P lost from agricultural fields can become an environmental pollutant, disturbing P-limited aquatic ecosystems.

**Soil organic matter (SOM) adds another layer of complexity to these interactions.** Organic acids released during the decomposition of SOM can compete with phosphate for the same adsorption sites on mineral surfaces, which can increase P concentrations in the soil solution. Furthermore, humic substances can form stable complexes with cations like  $Al^3$  and  $Fe^3$ , preventing them from precipitating phosphate and thereby enhancing its availability. The efficacy of P fertilization is often low due to these rapid and competing immobilization processes, and P lost from agricultural fields can become an environmental pollutant, disturbing P-limited aquatic ecosystems.

### 2.2 From Static Measurements to Dynamic Understanding

To manage this challenge, traditional soil testing methods (e.g., Olsen-P, AAE10, CO<sub>2</sub>-water) were developed to quantify the **size of the readily available P pool**. This static measurement is often referred to as the “**capacity factor**”. While these tests are invaluable for basic fertility assessment, they do not capture the dynamic nature of P supply. A crucial missing piece of information is the rate at which P is replenished into the soil solution from the solid phase after being taken up

by plant roots. This replenishment rate, or “**kinetic factor**”, is vital for sustaining crop growth, especially during periods of high demand.

The importance of these dynamics is not a new concept. As early as 1982, **Flossmann and Richter** argued that characterizing the kinetics of P release was essential for refining fertilizer recommendations beyond what static tests alone could offer. Modern research has reinforced this view, showing that fertilization strategies based solely on maintaining a critical soil test P (STP) concentration can be inefficient. In Switzerland, this has led to the accumulation of “legacy P” in many agricultural soils, and understanding the release kinetics of this legacy P is key to both improving nutrient efficiency and protecting water quality. Furthermore, critical STP levels are not constant; they are influenced by pedoclimatic factors like soil texture and temperature, making a “one-size-fits-all” approach to fertilization suboptimal.

## 2.3 Objectives and Research Questions

An ideal set of parameters for P management should meet several criteria. The parameters should correlate strongly with P export and P balance in a steady-state system. They must also respond to fertilizer inputs and, most importantly, capture the diffusive, kinetic nature of P supply to plant roots.

This thesis hypothesizes that **kinetic parameters describing P desorption, derived from a simple laboratory extraction, can serve as effective predictors for agronomic outcomes**. Using soils from the long-term STYCS experiment in Switzerland, this study employs a modified version of the Flossmann & Richter kinetic test to derive the desorption rate ( $k$ ) and the desorbable P pool ( $P_{desorb}$ ). The performance of these new kinetic parameters will be compared against standard STP methods ( $P_{CO_2}$  and  $P_{AAE10}$ ) by addressing the following research questions:

1. Is the P desorption kinetic method replicable and effective for the soils from the STYCS trial?
2. How do the kinetic coefficients,  $k$  and  $P^S$ , correlate with key soil properties (organic carbon, clay content, pH)?
3. How well do the standard STP methods ( $P_{CO_2}$  &  $P_{AAE10}$ ) predict crop yield, P export, and P balance?
4. Can the kinetic parameters,  $k$  and  $P^S$ , improve the prediction of these agronomic outcomes compared to the standard static tests?

## 3 Materials and Methods

### 3.1 The Long-Term Phosphorus Fertilization Experiment

The soil samples for this thesis originate from a set of six long-term field trials in Switzerland, established by Agroscope between 1989 and 1992. The primary objective of these experiments was to validate and re-evaluate Swiss phosphorus (P) fertilization guidelines by assessing long-term crop yield responses to varying P inputs across different pedoclimatic conditions. A detailed description of the experimental design and site characteristics can be found in (Hirte et al., 2021)

The experiment was set up as a **completely randomized block design** with four field replications at each site. The core of the experiment consists of six fixed-plot treatments representing different P fertilization levels, which were applied annually as superphosphate before tillage and sowing. These levels were based on percentages of the officially recommended P inputs: 0% (Zero), 33% (Deficit), 67% (Reduced), 100% (Norm), 133% (Elevated), and 167% (Surplus).

### 3.2 Experimental Sites

The six experimental sites are located in the main crop-growing regions of Switzerland: **Rümlang-Altwi (ALT)**, **Cadenazzo (CAD)**, **Ellighausen (ELL)**, **Grabs (GRA)**, **Oensingen (OEN)**, and **Zurich-Reckenholz (REC)**. The key soil properties are summarized below.

**Table 1:** Soil characteristics of the six long-term experimental sites. Data adapted from Hirte et al. (2021).

Site	Soil Type (WRB)	Clay (%)	Sand (%)	Organic C (g/kg)	pH (H2O)
ALT	Calcaric Cambisol	22	48	21	7.9
CAD	Eutric Fluvisol	8	40	14	6.3
ELL	Eutric Cambisol	33	31	23	6.6
GRA	Calcaric Fluvisol	17	34	16	8.3
OEN	Gleyic-calc. Cambisol	37	32	24	7.1
REC	Eutric Gleysol	39	25	27	7.4

Source: [Article Notebook](#)

Soil samples for this thesis were collected on [Your Sampling Date] from the topsoil layer (0-20 cm). [Add any further specific details about your sampling strategy here].

### 3.3 Phosphorus Desorption Kinetics

The analysis of phosphorus (P) desorption kinetics was based on the principles of sequential extraction established by Flossmann and Richter (1982). The original method is described below, followed by the specific protocol adapted for this study.

#### 3.3.1 Original Method of Flossmann and Richter (1982) {#sec-original-method-of-flossmann-and-richter-(1982)}

The foundational method aims to characterize the P replenishment capacity of the soil. The procedure is as follows:

1. **Removal of Soluble P:** 17.5 g of air-dried soil is shaken with 350 ml of deionized water for one hour at  $25 \pm 1^\circ\text{C}$ . The suspension is centrifuged and the supernatant is decanted to remove the readily soluble P fraction. This first extract is referred to as:
  - **Solution A:** Contains easily soluble P, which is discarded.
2. **Kinetic Extraction:** The remaining soil pellet is resuspended with another 350 ml of deionized water. Subsamples of the suspension are taken at specific time intervals, yielding the following extracts for kinetic analysis:
  - **Solution B:** Subsample taken after **10 minutes**.
  - **Solution C:** Subsample taken after **30 minutes**.
  - **Solution D:** Subsample taken after **120 minutes**.
3. **Analysis:** The P concentration in Solutions B, C, and D is determined colorimetrically using the molybdenum blue method according to Murphy and Riley (1962).

#### 3.3.2 Adapted Kinetic Protocol for This Study

For this thesis, the original method was modified to capture the desorption process with a higher temporal resolution and using a different soil-to-solution ratio.

1. **Soil Suspension:** 10 g of air-dried soil was suspended in 200 ml of deionized water. Unlike the original protocol, a pre-washing step to remove soluble P was not performed, meaning the measured desorption includes both the release of readily soluble P and the subsequent replenishment from the solid phase.
2. **Kinetic Extraction:** The suspension was shaken continuously, and subsamples were taken at eight time points to generate a detailed kinetic curve. The resulting extracts were:
  - **Extract 1:** Subsample taken after **2 minutes**.

- **Extract 2:** Subsample taken after **4 minutes**.
  - **Extract 3:** Subsample taken after **10 minutes**.
  - **Extract 4:** Subsample taken after **15 minutes**.
  - **Extract 5:** Subsample taken after **20 minutes**.
  - **Extract 6:** Subsample taken after **30 minutes**.
  - **Extract 7:** Subsample taken after **45 minutes**.
  - **Extract 8:** Subsample taken after **60 minutes**.
3. **Analysis:** Each subsample was immediately filtered. The concentration of orthophosphate in the filtered extracts was determined colorimetrically using the **malachite green method**.

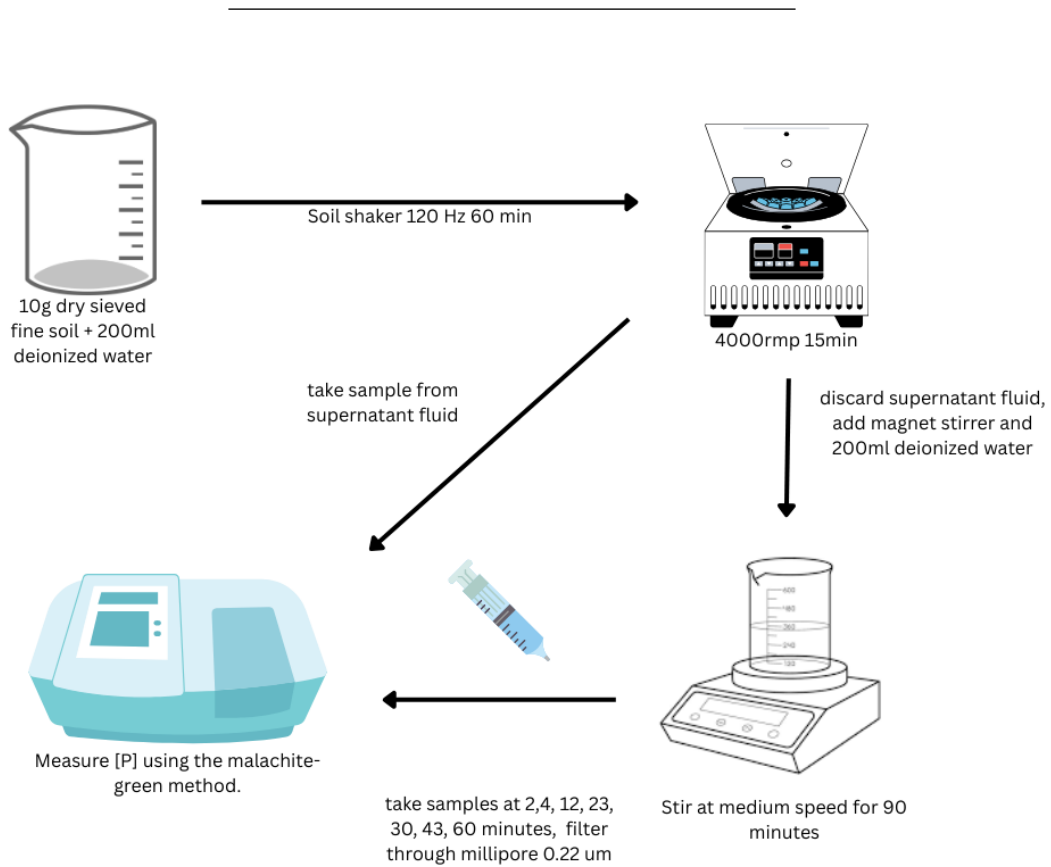


**Figure 1:** Flow-chart of the adapted Kinetik-experiment after Flossmann & Richter.

### 3.4 Statistical Analysis

The statistical workflow involved two main stages: 1) estimating the P desorption kinetic parameters from the laboratory data, and 2) using these parameters to model the agronomic outcomes from the long-term field experiment.

#### 3.4.1 Modeling of Desorption Kinetics

To derive the kinetic parameters, a non-linear mixed-effects model (**nlme**) was implemented. This approach was chosen to simultaneously estimate the rate constant ( $k$ ) and the maximum desorbable P ( $P_{desorb}$ ) directly from the time-series data for each soil sample. The model was fitted to the exact solution of the first-order rate equation:



$$P(t) = P_{desorb} \times (1 - e^{-k \times t'})$$

Where  $P(t)$  is the P concentration at time  $t$ , and  $t'$  is an adjusted time ( $t_{\min} + 3 \text{ min}$ ) to account for rapid initial P dissolution. The overall means for  $P_{desorb}$  and  $k$  were modeled as **fixed effects**, while sample-specific deviations for both parameters were modeled as **random effects** to capture the unique characteristics of each soil sample.

### 3.4.2 Modeling of Agronomic Responses

The estimated kinetic parameters were merged with the agronomic and soil chemistry dataset from the years 2017-2022. A series of linear mixed-effects models were then constructed to evaluate the predictive power of these parameters.

#### 3.4.2.1 Variables Used in the Models

The response and predictor variables used in the linear mixed-effects models are defined in the table below.

**Table 2:** Description of variables used in the agronomic models.

Abbreviation	Full.Name	Role	Description
$Y_{rel}$	Relative Yield	Response	Plot yield normalized by the national mean yield for that year and crop.
$Y_{norm}$	Normalized Yield	Response	Plot yield normalized by the site-specific median yield of the highest P treatment for that year and crop.
$P_{up}$	P Uptake	Response	Total P removed by the harvested crop biomass over a growing season ( $\text{kg P ha}^{-1}$ ).
$P_{bal}$	P Balance	Response	Net P budget, calculated as P inputs (fertilizer) minus P outputs (uptake) ( $\text{kg P ha}^{-1}$ ).
$k$	Rate Constant	Predictor	First-order rate constant of P desorption, representing the speed of P release ( $\text{min}^{-1}$ ).
$P_{desorb}$	Desorbable P	Predictor	Maximum desorbable P, representing the size of the readily available P pool ( $\text{mg P L}^{-1}$ ).
$J_0$	Initial P Flux	Predictor	Product of $k$ and $P_{desorb}$ , representing the initial flux of P from the soil.
$P_{CO2}$	Water-Soluble P	Predictor	Plant-available P measured by the $\text{CO}_2$ -saturated water extraction method ( $\text{mg P kg}^{-1}$ ).
$P_{AAE10}$	Chelate-Extractable P	Predictor	Plant-available P measured by the ammonium-acetate-EDTA extraction method ( $\text{mg P kg}^{-1}$ ).

Source: [Article Notebook](#)

#### 3.4.2.2 Linear Mixed-Effects Model Structure

Linear mixed-effects models (`lmer`) were used to test the relationships between the predictor variables and each of the three response variables. The structure of these models was designed to account for the nested nature of the long-term experiment. A general form of the model is:

*Response Variable*  $\sim$  *Fixed Effects* + (*1* | *Random Effects*)

- **Fixed Effects:** These represent the main explanatory variables of interest whose effects we wanted to quantify. The fixed effects included the kinetic parameters ( $k$ ,  $P_{desorb}$ ,  $J_0$ ) and the standard soil P tests ( $P_w$ ,  $P_{AAE10}$ ), along with their interactions.

- **Random Effects:** These were included to control for non-independence among observations. By including (1 | Site), (1 | Year), and (1 | Crop) as random intercepts, the model accounts for baseline differences in the response variable that are attributable to the specific location, growing season, or crop type, allowing for a more accurate estimation of the fixed effects.

To identify the most informative and parsimonious model, a systematic feature selection process was conducted using the `mlr3` machine learning framework. This involved training and evaluating different combinations of predictor variables using nested cross-validation to ensure the robustness of the final selected model.

All statistical analyses were performed in the R environment, utilizing the `nlme` package for kinetic modeling and the `lme4`, `lmerTest`, and `mlr3` packages for the final agronomic modeling and feature selection.

## 4 Results

Source: [Article Notebook](#)

The results of this study are presented in two main parts. First, the development and validation of the phosphorus (P) desorption kinetic model are detailed, justifying the final modeling approach. Second, the descriptive trends of both agronomic outcomes and soil P parameters in response to long-term fertilization and site differences are explored visually. Finally, the predictive power of the kinetic and standard P parameters is formally evaluated using linear mixed-effects models.

### 4.1 Establishment of the P-Desorption Kinetic Model

The primary goal was to derive two key parameters for each soil sample: the desorbable P pool ( $P_{desorb}$ ) and the rate constant ( $k$ ). The analysis proceeded in two stages: an initial test of a linearized model, followed by the implementation of a more robust non-linear model.

#### 4.1.1 Initial Approach: Failure of the Linearized Model

Following the conceptual framework of Flossmann and Richter (1982), the first-order kinetic equation was linearized. A core assumption of this model is that the linear relationship must pass through the origin. To test this, linear models were fitted to the transformed data for each sample individually. The results revealed a systematic failure of this assumption, as the estimated intercepts for the majority of samples were highly significantly different from zero ( $p < 0.05$ ). This consistent statistical deviation indicated that the linearized approach was not a valid representation of the data. The visual evidence in Figure 2 supports this conclusion.

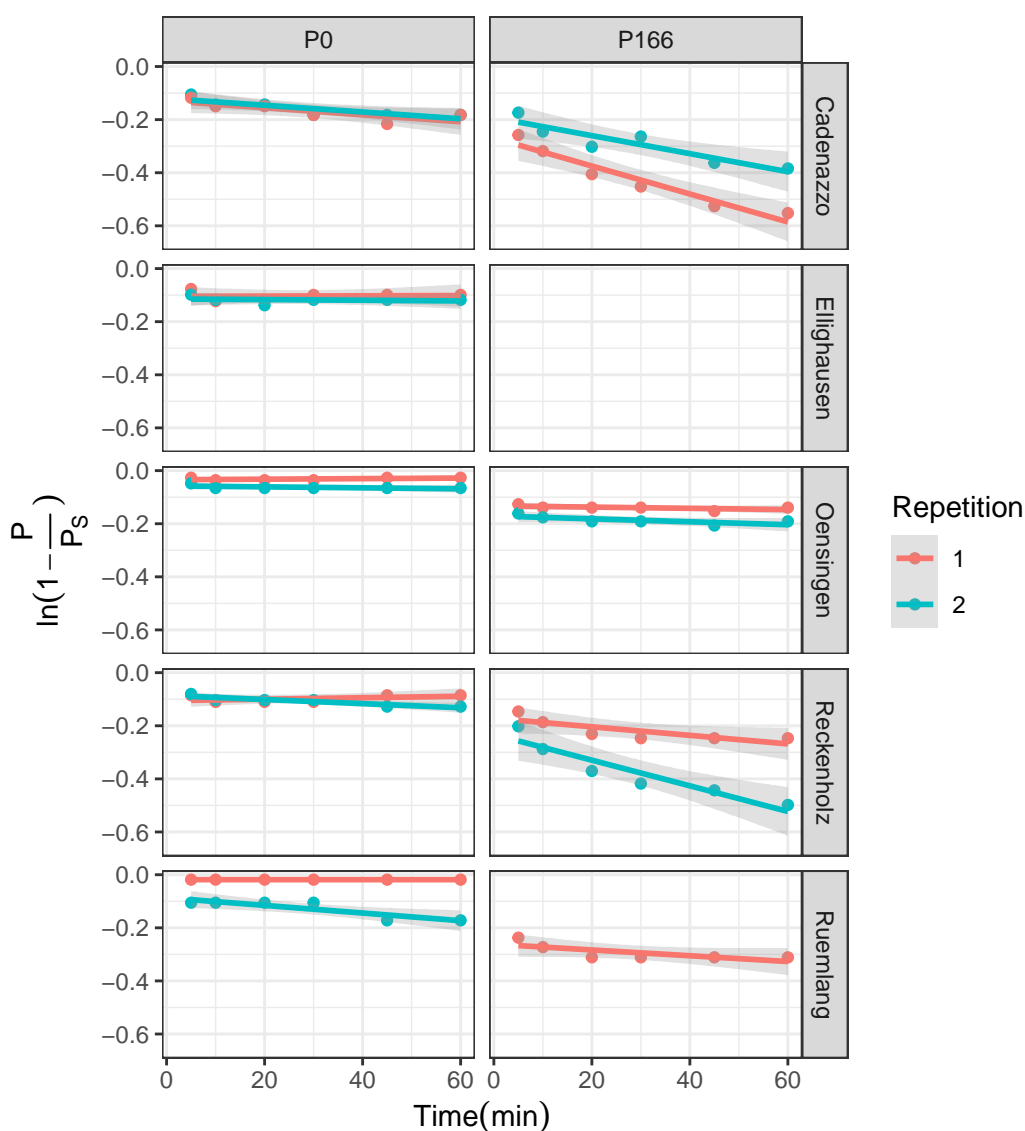


**Figure 2:** Test of the linearized first-order kinetic model. The plot visually supports the statistical finding that many intercepts are not zero.

Source: [Article Notebook](#)

#### 4.1.2 Final Approach: Successful Non-Linear Model

Given the statistical failure of the linearized model, a direct non-linear modeling approach was adopted to estimate both  $P_{desorb}$  and  $k$  simultaneously from the untransformed data. This approach does not rely on the assumption of a zero intercept and proved to be far more successful, accurately capturing the curvilinear shape of the desorption data for nearly all samples (fig-nonlinear-model). The final parameters were extracted from a non-linear mixed-effects model (`nlme`) to account for the hierarchical data structure. **These final nlme-derived coefficients were used for all subsequent analyses.**

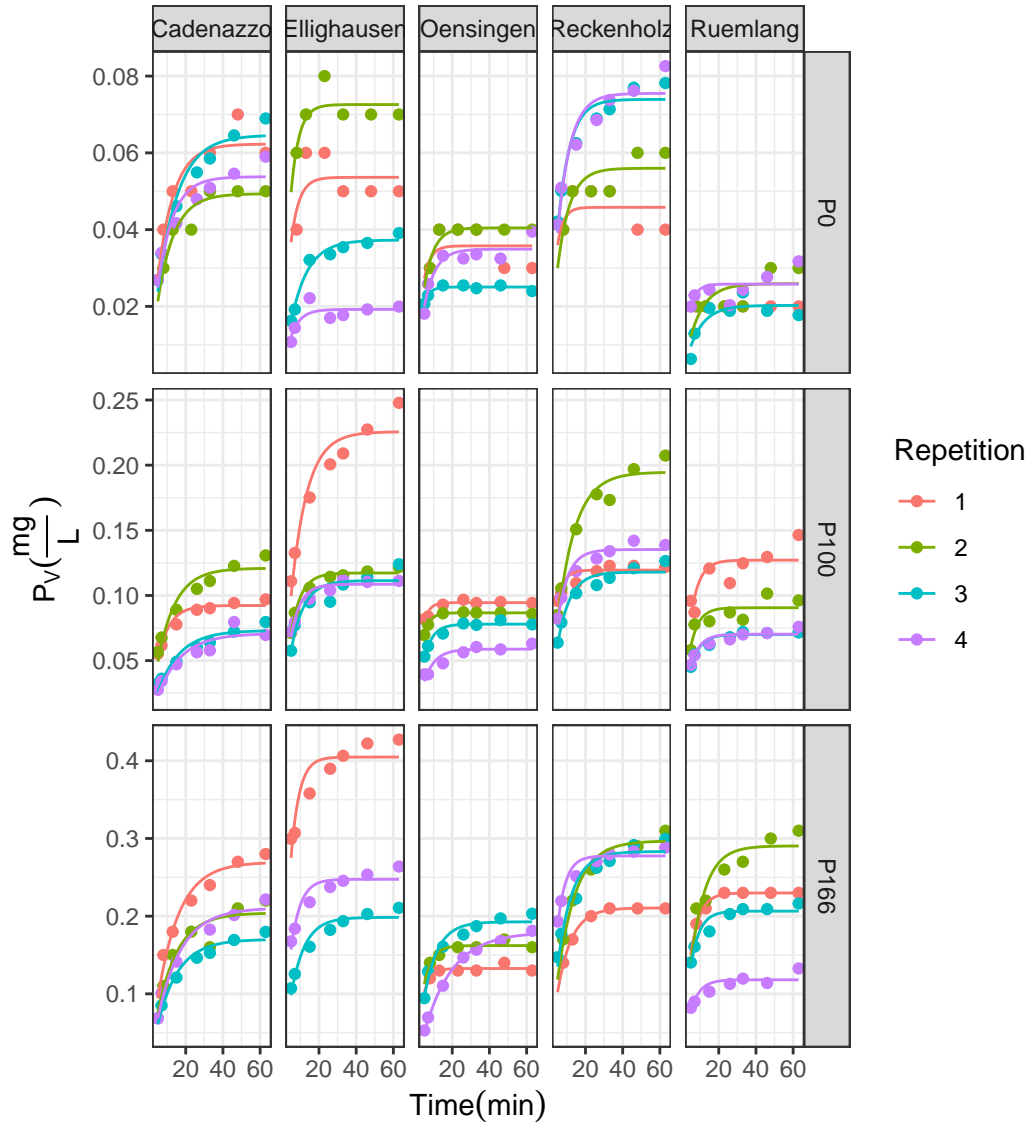


**Figure 3:** Non-linear first-order kinetic model fits for P desorption over time. Points represent measured data and solid lines represent the fitted model for each replicate.

Source: [Article Notebook](#)

## 4.2 Comparison with Isotopic Exchange Kinetics (IEK) {#sec-comparison-with-isotopic-exchange-kinetics-(iek)}

To validate the newly derived kinetic parameters against an established benchmark, the capacity ( $P_{desorb}$ ) and kinetic ( $k$ ) parameters were compared to data from Isotopic Exchange Kinetics (IEK) studies previously conducted on the same long-term trial sites by Demaria et al. (2013). This comparison aims to determine if the simpler, non-equilibrium desorption method used in this thesis captures similar aspects of soil P dynamics as the more complex, equilibrium-based IEK method.

The size of the desorbable P pool ( $P_{desorb}$ ) was compared against the long-term isotopically exchangeable P pool measured after 7 days ( $E_{exp\_10080}$ ). The desorption rate constant ( $k$ ) was compared against the IEK kinetic parameter measured after 24 hours ( $n_{1440}$ ). Spearman's rank correlation was used to robustly test for monotonic trends between the different methods.

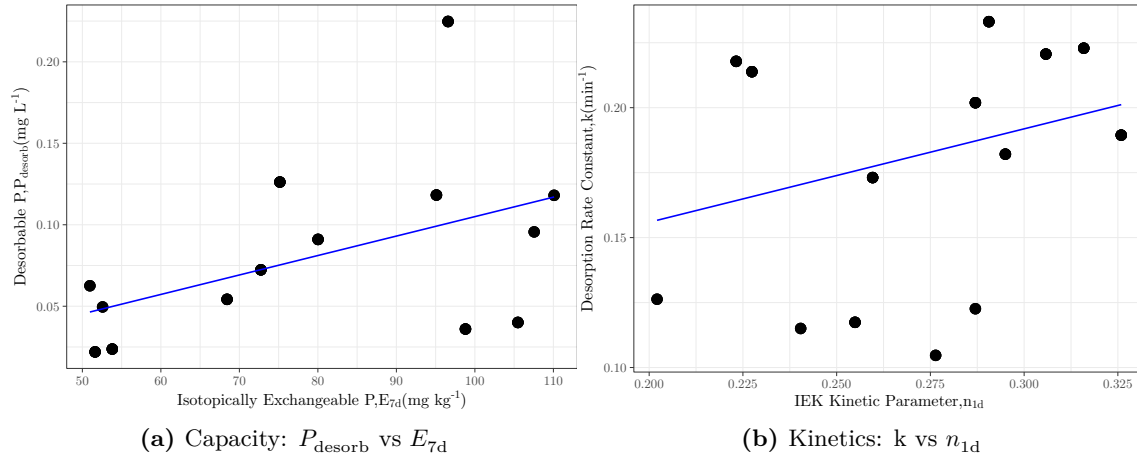


**Figure 4:** Correlation between desorption-derived kinetic parameters and IEK-derived parameters. (A) Capacity parameters: Desorbable P ( $P_{desorb}$ ) vs. Isotopically Exchangeable P ( $E_{7d}$ ). (B) Kinetic parameters: Rate Constant ( $k$ ) vs. IEK kinetic parameter ( $n_{1d}$ ).

The analysis revealed a statistically significant, moderate positive correlation between the capacity parameters,  $P_{desorb}$  and  $E_{exp\_10080}$  (fig-iek-comparison). The Spearman's rank correlation coefficient was 0.4 with a p-value of  $< 0.001$ .

Similarly, a statistically significant, moderate positive correlation was found between the kinetic parameters,  $k$  and  $n_{1440}$  (fig-iek-comparison). The Spearman's rank correlation coefficient was 0.36 with a p-value of  $< 0.001$ .

These results indicate that the simpler, non-equilibrium desorption method used in this study successfully captures both the capacity and intensity aspects of soil P lability, providing results that are consistent with the more complex, equilibrium-based IEK method reported by Demaria et al. (2013).

### 4.3 Effects of Fertilization on Agronomic and Soil Parameters

Having established a robust method to determine the kinetic parameters, the next step was to explore the effects of the long-term P fertilization treatments on both the agronomic outcomes and the soil P test parameters.

#### 4.3.1 Agronomic Responses to P Fertilization

The long-term application of different P fertilization levels had a pronounced impact on the primary agronomic outcomes, including two different metrics for yield, P Uptake ( $P_{up}$ ), and P Balance ( $P_{bal}$ ), though the response varied considerably between sites (Figure 5).

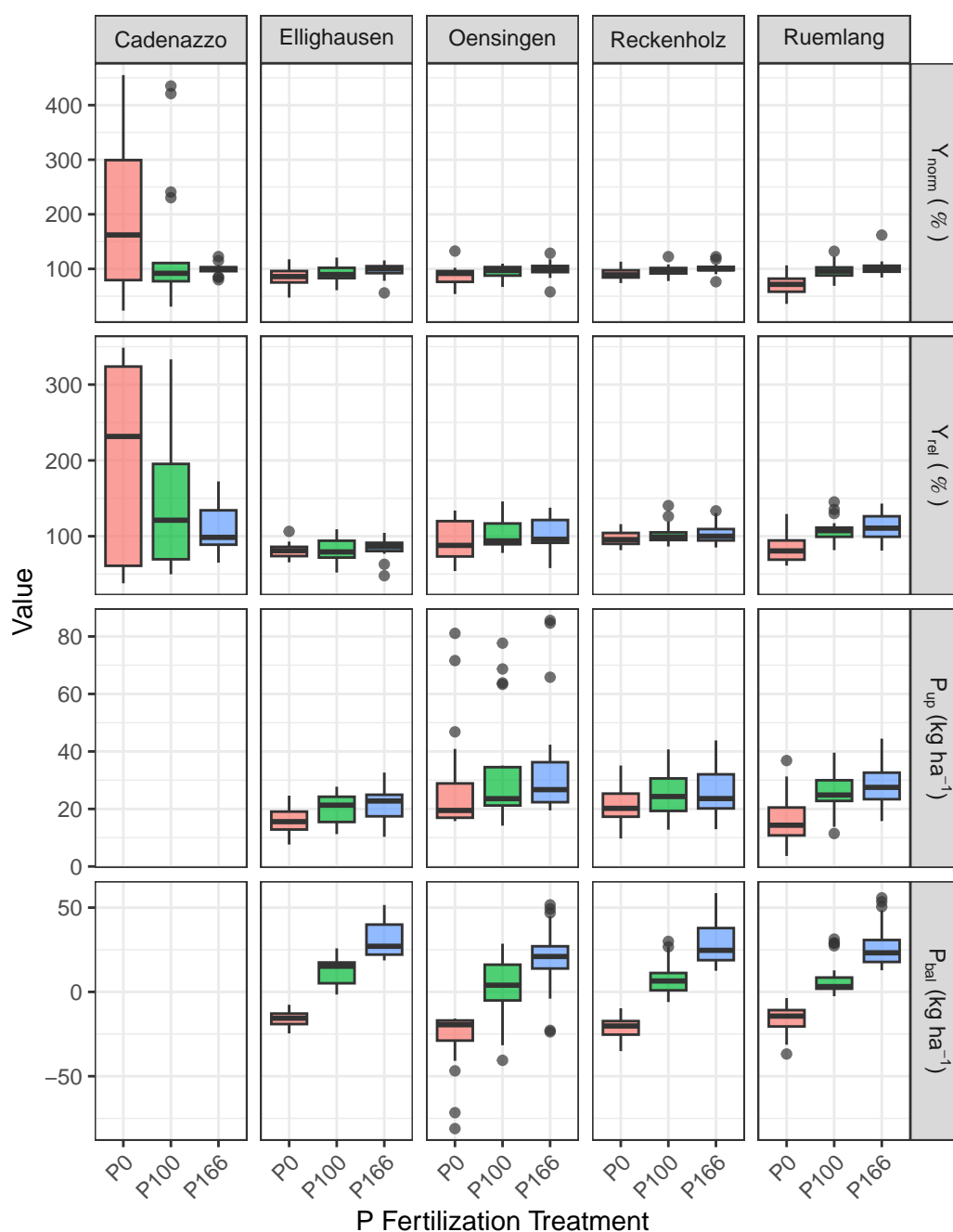


**Figure 5:** Agronomic response variables across six P fertilization treatments and six experimental sites. Data from 2017-2022.

Source: [Article Notebook](#)

**Yield Metrics ( $Y_{norm}$  and  $Y_{rel}$ ):** Both yield metrics showed a generally positive response to P fertilization. The site-normalized yield ( $Y_{norm}$ ) shows the response relative to the site's potential for that year, with most yields plateauing around the Norm (100%) treatment. The national-normalized yield ( $Y_{rel}$ ) provides a broader context, showing how yields at each site compare to the national average.

**P Uptake ( $P_{up}$ ):** P uptake by crops followed a similar trend to yield, increasing with fertilization, often continuing to increase at the highest fertilization levels, suggesting luxury consumption.

**P Balance ( $P_{bal}$ ):** The P balance showed a strong, linear relationship with fertilization. The Zero and Deficit treatments resulted in a negative balance (mining soil P), while the Elevated and Surplus treatments led to a significant P surplus.

#### 4.3.2 Soil P Parameters as a Function of P Fertilization

The different soil P test parameters, including the standard STP methods and the newly derived kinetic parameters, all responded to the long-term fertilization treatments (Figure 6).

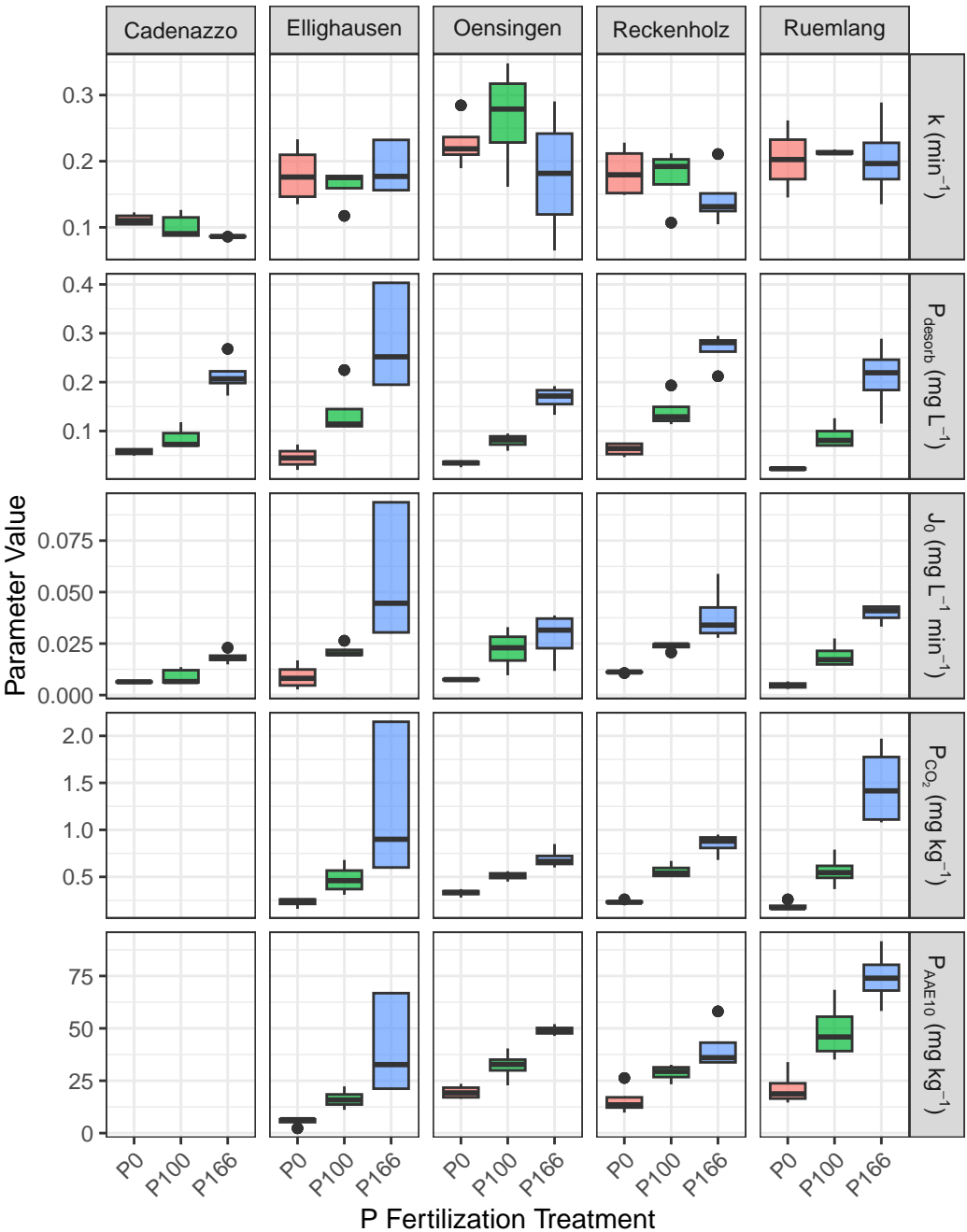


**Figure 6:** Soil P parameters across six P fertilization treatments and six experimental sites.

**Standard STPs** ( $P_{CO_2}$  and  $P_{AAE10}$ ): Both standard soil P tests showed a clear and consistent increase with rising P fertilization levels across all sites, confirming their sensitivity to management.

**Kinetic Parameters** ( $k$ ,  $P_{desorb}$ , and  $J_0$ ): \* **Desorbable P** ( $P_{desorb}$ ): This parameter behaved very similarly to the standard STPs, increasing steadily with P fertilization and confirming its role as a “capacity” indicator. \* **Rate Constant** ( $k$ ): The rate constant showed a more complex pattern, with no strong, consistent trend with fertilization. This suggests that while fertilization increases the *amount* of available P, it may not change the intrinsic *release rate*. \* **Initial P Flux** ( $J_0$ ): As the product of  $P_{desorb}$  and  $k$ , this parameter integrates both capacity and intensity. It showed a strong positive response to fertilization, driven primarily by the increase in  $P_{desorb}$ .

These initial observations suggest that the kinetic parameters, particularly the rate constant  $k$ , may provide unique information about the soil’s P dynamics not captured by static tests alone. The next section will use formal statistical models to test these relationships.

#### 4.4 Predicting P Parameters from Soil Properties

To understand the underlying drivers of the standard and kinetic P parameters, a series of linear mixed-effects models were fitted. Each model predicted one of the P parameters based on the core soil properties: organic carbon ( $C_{org}$ ), clay content, silt content, pH, and amorphous Al/Fe oxides. The models included random effects for **Site**, **Year**, and **Block**. The results are summarized in Table 3.

**Table 3:** Results of linear mixed-effects models predicting P parameters from intrinsic soil properties. Significance codes: ‘’  $p < 0.001$ , ’’  $p < 0.01$ , ’’  $p < 0.05$ .

Model	$P_{desorb}$	$k$	$J_0$	$P_{CO_2}$	$P_{AAE10}$
Intercept	21.444***	0.454	21.189***	14.014**	23.126**
Ald	-8.706***	-0.072	-8.631*	-4.417	-9.473*
Fed	-1.068***	0.005	-1.084	-0.845*	-0.606
Clay	-0.006	-0.016**	-0.085	0.015	-0.029
$C_{org}$	0.612*	0.137**	1.250*	0.269	1.454***
pH	-0.018	-0.021	-0.092	0.124	0.012
Silt	-0.000	0.004	0.008	-0.015	-0.049*
$R_m^2$	0.393	0.212	0.368	0.362	0.494
$R_c^2$	0.996	0.915	0.993	0.995	0.997

Source: [Article Notebook](#)

The analysis in Table 3 reveals that the capacity-based P pools and the kinetic rate constant are controlled by different sets of soil properties. Both amorphous aluminum ( $Al_{ox}$ ) and iron ( $Fe_{ox}$ ) oxides had a highly significant negative effect on the **Desorbable P pool** ( $P_{desorb}$ ), suggesting they bind P strongly. In contrast, **Organic Carbon** ( $C_{org}$ ) had a significant positive effect on all capacity measures, especially  $P_{AAE10}$ . The **Rate Constant** ( $k$ ) was not significantly driven by the oxides, but showed a significant positive relationship with  $C_{org}$  and a negative relationship with Clay content, indicating that the speed of P release is governed by different mechanisms than the total pool size.

#### 4.5 Predictive Modeling of Agronomic Outcomes

To formally evaluate and compare the predictive power of the standard STP methods against the newly derived kinetic parameters, a series of linear mixed-effects models (`lmer`) were fitted for each of the primary agronomic response variables.



#### 4.5.1 Predicting Site-Normalized Yield ( $Y_{norm}$ )

The models predicting the site-normalized yield are summarized in Table 4. For this metric, the standard STP methods proved to be the most effective predictors.

**Table 4:** Results of linear mixed-effects models predicting Site-Normalized Yield ( $Y_{norm}$ ).

Model	$Y_{norm} \sim P_{CO_2}$	$Y_{norm} \sim P_{AAE10}$	$Y_{norm} \sim P_{CO_2} * P_{AAE10}$	$Y_{norm} \sim k * P_{desorb}$
Intercept	1.059***	0.532***	1.096***	0.980
$k$				2.262
$J_0$				0.931
$\log(P_{desorb})$				-0.063
$\log(P_{AAE10})$		0.120***	-0.006	
$\log(P_{CO_2})$	0.162***		0.137	
$P_{CO_2} \times P_{AAE10}$			0.016	
$R_m^2$	0.218	0.198	0.220	0.014
$R_c^2$	0.358	0.474	0.365	0.360

Source: [Article Notebook](#)

As shown in Table 4, both  $P_{CO_2}$  and  $P_{AAE10}$  were highly significant predictors of site-normalized yield, with the model containing  $P_{CO_2}$  explaining the most variance (Marginal  $R^2 = 0.218$ ). In contrast, the kinetic parameters showed no significant predictive power for  $Y_{norm}$ .

#### 4.5.2 Predicting National-Normalized Yield ( $Y_{rel}$ )

When predicting the yield normalized to the national average, the kinetic parameters demonstrated a much stronger performance, as summarized in Table 5.

**Table 5:** Results of linear mixed-effects models predicting National-Normalized Yield ( $Y_{rel}$ ).

Model	$Y_{rel} \sim P_{CO_2}$	$Y_{rel} \sim P_{AAE10}$	$Y_{rel} \sim P_{CO_2} * P_{AAE10}$	$Y_{rel} \sim k * P_{desorb}$
Intercept	104.862***	75.343***	130.274***	56.375
$k$				377.498**
$J_0$				171.507**
$\log(P_{desorb})$				-27.486*
$\log(P_{AAE10})$		7.111**	-6.537	
$\log(P_{CO_2})$	8.853**		23.091	
$P_{CO_2} \times P_{AAE10}$			-3.110	
$R_m^2$	0.074	0.063	0.078	0.022
$R_c^2$	0.569	0.537	0.596	0.439

Source: [Article Notebook](#)

As seen in Table 5, while the standard STP methods were also significant predictors, the kinetic model revealed a significant positive effect of the **Rate Constant** ( $k$ ) and its interaction with  $P_{desorb}$  ( $J_0$ ). This suggests that the speed of P release is a more important factor when comparing yields across the broader environmental gradient represented by the national average.

#### 4.5.3 Predicting P-Export ( $P_{up}$ )

For predicting P-Export, the standard STP methods performed very well, with the kinetic model showing comparable, albeit non-significant, performance, as shown in Table 6.

**Table 6:** Results of linear mixed-effects models predicting P-Export ( $P_{up}$ ).

Model	$P_{up} \sim P_{CO_2}$	$P_{up} \sim P_{AAE10}$	$P_{up} \sim P_{CO_2} * P_{AAE10}$	$P_{up} \sim k * P_{desorb}$
Intercept	27.522***	8.090	30.632*	29.599***
$k$				22.622
$J_0$				11.928
$\log(P_{desorb})$				1.954
$\log(P_{AAE10})$		4.824***	-0.805	
$\log(P_{CO_2})$	5.177***		8.069	
$P_{CO_2} \times P_{AAE10}$			-0.814	
$R_m^2$	0.064	0.073	0.065	0.064
$R_c^2$	0.625	0.603	0.623	0.648

Source: [Article Notebook](#)

The results in Table 6 show that both  $P_{CO_2}$  and  $P_{AAE10}$  were highly significant predictors, explaining around 6-7% of the variance (marginal  $R^2$ ). This suggests that the size of the available P pool is a robust indicator of the amount of P a crop will take up.

#### 4.5.4 Predicting P-Balance ( $P_{bal}$ )

The most striking result was found when predicting the P-Balance, summarized in Table 7. The standard STP methods showed no significant ability to predict the P-Balance, whereas the kinetic model was a powerful predictor.

**Table 7:** Results of linear mixed-effects models predicting P-Balance ( $P_{bal}$ ).

Model	$P_{bal} \sim P_{CO_2}$	$P_{bal} \sim P_{AAE10}$	$P_{bal} \sim P_{CO_2} * P_{AAE10}$	$P_{bal} \sim k * P_{desorb}$
Intercept	4.441	7.691	3.649	43.833***
$k$				84.993
$J_0$				33.029
$\log(P_{desorb})$				16.947***
$\log(P_{AAE10})$		-0.794	0.187	
$\log(P_{CO_2})$	-0.928		-2.442	
$P_{CO_2} \times P_{AAE10}$			0.462	
$R_m^2$	0.001	0.001	0.001	0.572
$R_c^2$	0.810	0.807	0.811	0.744

Source: [Article Notebook](#)

As detailed in Table 7, the kinetic model explained **57% of the variance** in P-Balance (marginal  $R^2 = 0.572$ ), with the **Desorbable P pool** ( $P_{desorb}$ ) being the dominant, highly significant predictor. This indicates that the  $P_{desorb}$  parameter from the kinetic experiment is a vastly superior measure of the soil's P budget compared to standard STP tests.

## **5 Discussion**

## **6 Conclusion**

## **7 Acknowledgments**

## **8 Legal Disclosure**

## **9 References**

Hirte, J., Richner, W., Orth, B., Liebisch, F., & Flisch, R. (2021). Yield response to soil test phosphorus in switzerland: Pedoclimatic drivers of critical concentrations for optimal crop yields using multilevel modelling. *Science of The Total Environment*, 755, 143453. <https://doi.org/10.1016/j.scitotenv.2020.143453>

## **10 Appendix**

## **11 Supplements**



Eidgenössische Technische Hochschule Zürich  
Swiss Federal Institute of Technology Zurich

**Title of work:**

Master Thesis

**Thesis type and date:**

Master's Thesis,

**Supervision:**

Prof. Dr. Emmanuel Frossard  
Dr. Frank Liebisch

**Student:**

Name: Marc Jerónimo Pérez y Roperó  
E-mail: marcpe@ethz.ch  
Legi-Nr.: 13-938-311

**Statement regarding plagiarism:**

By signing this statement, I affirm that I have read and signed the Declaration of Originality, independently produced this paper, and adhered to the general practice of source citation in this subject-area.

Declaration of Originality:

[http://www.ethz.ch/faculty/exams/plagiarism/confirmation\\_en.pdf](http://www.ethz.ch/faculty/exams/plagiarism/confirmation_en.pdf)

Zurich, 7. 9. 2025:

*My Signature*